ACS APPLIED MATERIALS & INTERFACES

Research Article

www.acsami.org

Investigation of Ester- and Amide-Linker-Based Porous Organic Polymers for Carbon Dioxide Capture and Separation at Wide Temperatures and Pressures

Ruh Ullah,[†,#] Mert Atilhan,[*,†] Baraa Anaya,[†] Shaheen Al-Muhtaseb,[†] Santiago Aparicio,[‡] Hasmukh Patel,[§,#] Damien Thirion,[∥] and Cafer T. Yavuz[*,∥,⊥]

[†]Department of Chemical Engineering, Qatar University, PO Box 2713, Doha, Qatar

[‡]Department of Chemistry, University of Burgos, 09001 Burgos, Spain

[§]Department of Chemistry, Northwestern University, Evanston, Illinois 60208, United States

[∥]Graduate School of EEWS, KAIST, 373-1 Guseong Dong, Yuseong Gu, Daejeon 305-701, Republic of Korea

[⊥]Department of Chemistry, KAIST, 373-1 Guseong Dong, Yuseong Gu, Daejeon 305-701, Republic of Korea

Supporting Information

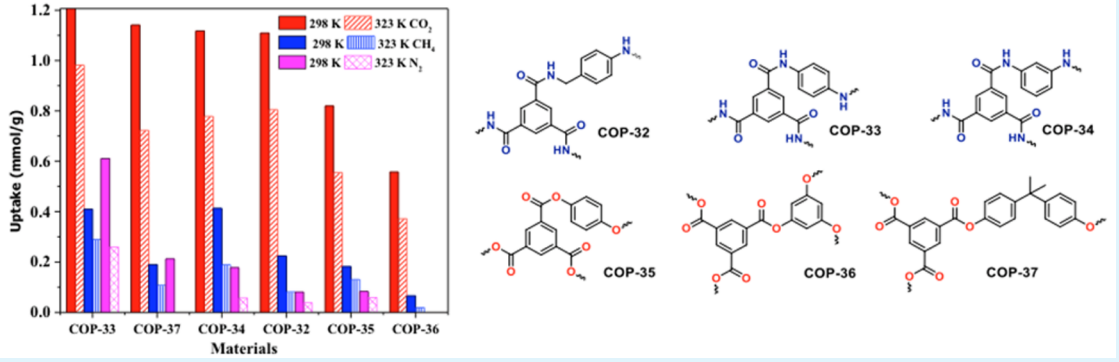

ABSTRACT: Organic compounds, such as covalent organic framework, metal−organic frameworks, and covalent organic polymers have been under investigation to replace the well-known amine-based solvent sorption technology of CO_2 and introduce the most efficient and economical material for CO_2 capture and storage. Various organic polymers having different function groups have been under investigation both for low and high pressure CO_2 capture. However, search for a promising material to overcome the issues of lower selectivity, less capturing capacity, lower mass transfer coefficient and instability in materials performance at high pressure and various temperatures is still ongoing process. Herein, we report synthesis of six covalent organic polymers (COPs) and their CO_2, N_2, and CH_4 adsorption performances at low and high pressures up to 200 bar. All the presented COPs materials were characterized by using elemental analysis method, Fourier transform infrared spectroscopy (FTIR) and solid state nuclear magnetic resonance (NMR) spectroscopy techniques. Physical properties of the materials such as surface areas, pore volume and pore size were determined through BET analysis at 77 K. All the materials were tested for CO_2, CH_4, and N_2 adsorption using state of the art equipment, magnetic suspension balance (MSB). Results indicated that, amide based material i.e. COP-33 has the largest pore volume of 0.2 cm^2/g which can capture up to the maximum of 1.44 mmol/g CO_2 at room temperature and at pressure of 10 bar. However, at higher pressure of 200 bar and 308 K ester-based compound, that is, COP-35 adsorb as large as 144 mmol/g, which is the largest gas capturing capacity of any COPs material obtained so far. Importantly, single gas measurement based selectivity of COP-33 was comparatively better than all other COPs materials at all condition. Nevertheless, overall performance of COP-35 rate of adsorption and heat of adsorption has indicated that this material can be considered for further exploration as efficient and cheaply available solid sorbent material for CO_2 capture and separation.

KEYWORDS: *CO_2 capture, porous adsorbents, covalent organic polymers, high-pressure capture*

1. INTRODUCTION

Sustainable and economical capture and separation of CO_2 from fossil fuel based industries is highly desirable to govern the excessive emission, mitigate the adverse anthropogenic effects and uphold the overall concentration of greenhouse gases up to

Received: May 18, 2016
Accepted: July 26, 2016
Published: July 26, 2016

DOI: 10.1021/acsami.6b05927
ACS Appl. Mater. Interfaces 2016, 8, 20772−20785

the UN recommended level.[1] In addition to the customarily used aqueous monoethanolamine systems, various other technologies and materials particularly solid sorbents[2] such as metal organic framework (MOF), covalent organic framework (COF),[3] activated carbon, mesoporous silicas, zeolites polybenzimidazole, inorganic materials, and many polymers[4] have been explored to overcome the issues of capturing capacity, reusability, selectivity and stability of the sorbents materials. Among various solid materials, organic polymers have the additional benefits of simple preparation, low manufacturing cost, abundant availability, nontoxicity, biodegradability and structure flexibility for capturing different gases at different environmental conditions.[4] Importantly, selection of the core monomers and linkers independently steer the physical properties as well as the structures of polymer networks. Literature in this field has the opinion that capturing route is mainly based on the physical sorption of the polymer materials which makes the process appropriate as long as the repeated useability of the solid sorbent is concern. This is still under debate in literature[2,5] that gas uptake capacity of solid sorbents apparently dependent on the physical parameters like surface area, pore volume and structure rigidity of the materials. On the other hand physical properties which steer the gas capturing capacity are hooked to the selection of core monomers and linkers in case of polymer networks. Various organic polymeric materials prepared from the same building block, but, linked by different chain linkers have significant differences in the nature of physical parameters.[6] For example microporous organic polymers (MOPs) prepared with benzene as core monomers and linked by two different agents 1,3,5-tris(bromomethyl)-2,4,6-trimethylbenzene and 1,3,5-tris(bromomethyl)benzene have different surface areas (609 and 688 m^2/g), pore volumes (0.35 and 0.40 cm^3/g), and different CO_2 adsorptions of 63.6 and 101 mg/g, respectively.[7] Covalent organic polymers (COPs) have been recently introduced as a new class of polymers compounds which have promising high CO_2 capturing capacity[8] mainly associated with the physical parameters of the materials. Cyanuric chloride based covalent organic polymers linked by piperazine and 4,4-bipiperidine have different surface areas of 168 and 158 m^2/g respectively, which consequently have significant effect on the adsorption capacity.[9] Liebl et al.[10] have reported that CO_2 capturing capacity of triazine-based porous polyimide (TPI) materials is mainly attributed to the combined effect of functionality of the surfaces and surface area of the network which can be tuned with the help of different linkers. It was further argued that the inflexible nature of the linkers at the center of materials in case of PTI-1 and PTI-2 as compared to the other polymer networks make the structures of these materials more rigid because of the covalent bonds[11] incorporated by the linkers. Beside the larger surface area and pore volume; physical sorbents materials should have attractive outer surface and inner pore surfaces to capture CO_2 from the stream of the flue gases. CO_2 affinity toward the attaching site can be established by enhancing the basicity and functionalization[12] of the capturing compounds. Sekiskardes et al.[13] have attempted to introduce the nitrogen functionality (basicity) in various types of polymers by incorporating imidazole ring as a linker within the structure of polymers, however, materials with the largest surface area has shown excellent performance as long as the capture capacity of the sorbent is concern. So far most of the related research has been focused on the investigation of capturing capacity and selectivity of organic polymers, however, minor attention has been made toward the rate of the adsorption process. In our knowledge and as per the literature survey excluding porous polymers only few lithium based composite materials[14] have been explored for the adsorption rate of CO_2. Kato et al.[15] has found that Li_4SiO_4 has the highest adsorption rate for CO_2, which could capture up to 50 mg/g/min at 500 °C using TGA analysis techniques. It might be possible that a sorbent can have larger capturing capacity as compared to other counterparts, however, due to slow adsorption kinetics, despite lower capture capacity other counterpart materials might be faster in adsorption process and could be advantageous in processes that requires rapid gas adsorption−desorption cycles. Adsorption−desorption kinetics has similar importance as the capacity of the materials, since; rapid removal[16] of the unwanted gas molecules is highly essential in some industrial processes[17] to avoid further chemical reaction and formation of toxic hazardous compounds. Here in it has been attempted to investigate the effect of nitrogen[18] and hydroxyl functionalities[19] independently on the CO_2, N_2, and CH_4 adsorption capacity and rate of adsorption by making two different sets i.e. amide[10,20] and ester based[11,21] COPs materials with two different core monomers and six different linkers. The objective of this work is to investigate the newly synthesized covalent organic polymers and their gas uptake performances considering various gases including CO_2, N_2, CH_4, and H_2.

2. EXPERIMENTAL SECTION

Materials and Methodology. *N,N*-Diisopropylethylamine, 1,3,5-benzene tricarbonyltrichloride, 4-aminobenzylamine, 1,4-phenylenediamine, 1,3-phenylenediamine, hydroquinone, phloroglucinol, bisphenol A were purchased from Sigma-Aldrich, and were used as received, however, dioxane, and ethanol were obtained from TCI, Japan.

In a typical synthesis (detailed experimental procedure given Supporting Information), *N,N*-diisopropylethylamine was added to linker (4-aminobenzylamine, 1,4-phenylenediamine, 1,3-phenylenediamine, hydroquinone, phloroglucinol, or bisphenol A) dissolved in 1,4-dioxane at room temperature. The dioxane solution of core (1,3,5-benzene tricarbonyltrichloride) was added dropwise to the above solutions with continuous stirring at 12−14 °C in the atmospheric condition. Once the addition was finished, the reaction mixture slowly heated up to room temperature and it was stirred for 24 h. The precipitate was washed with dioxane and soaked in ethyl alcohol three times over the period of 12 h. The obtained product, COPs-32−37, was dried at room temperature under vacuum for 2 h and subsequently was dried at 110 °C in vacuum for 5 h. Yield of the materials was measured to be in the range of 74−86%.

Elemental analysis was performed at Korea Advance Institute of Science and Technology (KAIST) Central Research Instrument Facility using Thermo Scientific FLASH 2000 equipped with a TCD detector and Bruker Advance 400 MHz WB equipped with a 4 mm probe. Solid-state 13C and 31P cross-polarization magic angle spinning NMR (CP-MAS) were conducted by spinning the samples at 12 kHz and 20 kHz respectively with the contact time of 5 ms and a delay time of 3 s. Fourier transform infrared spectra (FTIR) were recorded on a Shimadzu IR-Tracer-100 equipped with a Gladi ATR module. Morphological study of materials was conducted with scanning electron microscope (FE-SEM-Nova Nano-450, Netherland) where the samples were uniformly and directly coated on an aluminum stub having 3 nm platinum coating, which was used as a conducting material. Physical properties of polymers were determined with nitrogen adsorption isotherms using a Micrometrics 3FLEX accelerated surface area and porosimetry analyzer at 77 K. Prior to sorption measurement for physical parameters analysis, samples were activated through a degassing step at 423 K for 5 h under vacuum, which was applied by a mechanical roughing pump, manufactured by Varian Inc. The specific surface areas were derived from Brunauer−

DOI: 10.1021/acsami.6b05927
ACS Appl. Mater. Interfaces 2016, 8, 20772−20785

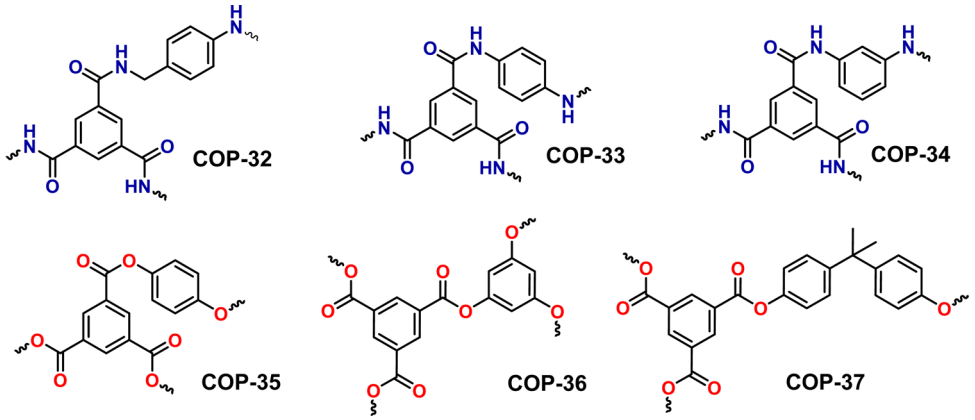

Figure 1. Repeating unit structure of amide and ester-linked covalent organic polymers (COPs-32−37).

Emmett−Teller (BET) method. Pore volume and pore diameter were determined via the BJH desorption model. FE-SEM (field emission scanning electron microscope) was taken using Nova 230 to study the structure of materials. Tapping density of the materials is measured with the help of AUTOTAP density analyzer from Quantachrome Instruments at the tapping rate of 2000 per hour. Prior to density measurement samples were dried in oven at 110 °C for 24 h to evacuate the materials from water content.

Thermal stability was studied with PerkinElmer Pyris 6 (Thermogravimetric Analysis) TGA machine, where materials were heated in N_2 environment from 30 to 800 °C at the rate of 3 °C per minute. On the other hand, in situ infrared Fourier transform spectroscopy (FTIR) was used to investigate the interaction of CO_2 with COP material through the in situ diffuse reflectance (DRIFTS) measurements techniques. Certain amounts of COPs materials were mixed with potassium bromide powder in a proper ratio to dilute the magnitude of materials under investigation. The solid mixture was then, degassed for at least 12 h using BET analysis system prior to in situ measurement. Diluted COP material was subjected to various pressures (0.1 to1 bar) ranges at 25 °C and data was collected for each pressure range. Pressure was applied manually, into the closed chamber containing diluted COPs materials. Spectra of COP material exposed to different pressures of CO_2 were collected after allowing at least 5 min for adsorption saturation. Background spectrum obtained with pure KBr detector in CO_2 environment was subtracted from the diluted samples spectrum to eliminate the contribution of CO_2 in the bulk.

Magnetic suspension balance (MSB) from Rubotherm Prazisions Messtechnik GmbH equipped with automated Teledyne Isco 260 D pump was used to measure the low and high pressure gas uptake of the synthesized sorbent materials and this apparatus is located at Qatar University laboratory. Details about experimental set up of MSB for high pressure gases measurement has been mentioned in literature previously.[22] However, in a typical procedure, fixed amount (0.10−0.2 g) of each sample was first evacuated for at least 12 h at 101 °C within the closed sample chamber of balance to completely eliminate the effect of humidity. Four gas cylinders high purity (grade-2) gas cylinders are connected to gas dosing system (GDS) via external pump to pressurize the required gas into the measuring cell. The maximum set pressure (10 for low pressure measurements and 200 bar for high pressure measurements) was applied stepwise by increasing the pressure gradually from 1 bar up to the maximum of 10 and 200 bar, respectively. Each pressure point took about 60 min to gain the set point of pressure and temperature equilibrium, recorded four different sets of measurements and collected the data points. In case of low pressure measurement each measurement point was taken after 1 bar increment reaching up to the maximum of 10 bar, totalling of 12 measurements including evacuation step of the cell at the beginning and at the final stage of the measurement cycle. For high-pressure measurement, data was collected by total of 21 measurement points including initial and final evacuation. Initially, pressure of the system was increased gradually from 5, 10, 15, and 25 bar with each step of 1 h and then each point was incremented with 25 bar reaching to 200 bar. After reaching the maximum set pressure points both in low and high pressure condition, pressure of the system was gradually reduced exactly with the same measurement points starting from the high pressure and reaching to the last evacuation point to complete the desorption process. The system is fully automated and the pressure goes to next higher point after completing the previous measurement point. The system was brought to atmospheric pressure subsequently by final evacuation of at least 5 h at the same temperature. The above procedure was repeated with the same sample (unchanged sample) each for three temperatures, that is, 308, 323, and 338 K and three gases (CO_2, N_2, and CH_4) with total evacuation of at least 10 h in each case. COPs samples were exposed to cyclic (at least 3 cycles per samples) adsorption/desorption experiments for observing the activity and performance of the materials.

Moreover, MSB apparatus is equipped with in situ density measurement capability and it is used for obtaining the density values for the gases that are processed in the experimental measurement cell during the adsorption measurements. To make sure the physical state of the measured gas and rule out possible condensation of the gases on the pores of the adsorbent material, the density of the gas is experimented in the MSB. Then this density data is crosschecked by using a NIST reference database for pure components via REFPROP 9.1 software.[23] Last but not least, the density data that is obtained from in situ measurements in the MSB and the calculated density values at high pressures by using REFPROP software is compared with published material for the pure gases that are used in this work and no ambiguity has been observed for the gas densities.[24]

3. RESULTS AND DISCUSSIONS

Figure 1, shows the schematics of amide and ester linked covalent organic polymers obtained with the procedure mentioned in the Materials and Methodology section. Organic polymers with two different (i.e., OH and N) functionalities were prepared with the objective to examine the effectiveness of two functionalities for large capacity and high selectivity CO_2 capture at various temperatures and pressures. Amides are proven to have high polarity while ester have good stability and therefore may have applications in high pressure CO_2 adsorption.[25] Thus, as shown in the schematic fundamental block, benzene tricarbonyltrichloride was linked by two different linkers, having nitrogen (amide) (COP-32, COP-33, and COP-34) and hydroxyl (ester) ions (COP-35, COP-36, and COP-37) functionality with in the repeating chain structures. COPs that are presented in this work are numbered in a consecutive way according previous publications.[9,26]

Elemental analysis of COPs materials (given in Table 1) shows the experimental percentage contents of carbon,

DOI: 10.1021/acsami.6b05927
ACS Appl. Mater. Interfaces 2016, 8, 20772−20785

Table 1. Elemental Analysis of COPs-32-37

material ID	C %	H %	N %	O %
COP-32	68.9	5.3	12	1.6
COP-33	67.4	5	13.8	1.6
COP-34	59.8	4.8	27.8	1.6
COP-35	66.1	3.6		29.9
COP-36	61.2	3.9		34.8
COP-37	75.8	5.4		19.5

hydrogen, nitrogen, and oxygen in these structures. Table 1 reveals that amides based polymers (COP-32, COP-33, and COP-34) have same concentration of O (1.6%), but carbon content is reducing from 68.9% to 59.8% as the concentration of N increases from 12% to 27.8% indicating strong interaction of linkers with parent monomer. The high content of nitrogen in COP-34 indicates that 1,3-phenylene is more reactive than 4-aminobenzylamine and 1,4-phenylene with tricarbonyltrichloride resulting in chain structures of COP-34. On the hand, ester linked polymers (COP-35, COP-36, and COP-37) have obviously more oxygen concentration than the amide type materials owing to the presence of hydroxyl moiety in the linkers molecules. Additionally, COP-37 has the highest concentration of carbon (75.8%) among all new materials with the least oxygen quantity (19.5) among the ester type chained covalent organic polymers. It is important to note that, COP-33 in amide series and COP-35 in ester series have the average carbon concentration of 67.4% and 66.1% respectively, with average content of nitrogen (13.8%) and oxygen (29.9%). Additionally, FTIR analysis (Figure 1, Supporting Information) confirmed formation of amides and ester based materials, since prominent peaks at 1530−1660, 1735, and 1220 cm^{-1} observed, which can be associated with N−H bending, C═O, and C−O stretching, respectively.[27] The two major peaks in the range of 1735 and 1300−1000 cm^{-1} indicates the presence of saturated aliphatic ester and carbonyl group.[28] The three prominent peaks in the range of 3400, 1615, and 1516 cm^{-1} in COP-32, COP-33, and COP-34 are attributed to the presence of the amino group, N−H stretching, and N−O stretching mode indicating formation of the required amide based materials.[29]

Thermal stability of the materials were tested by sintering materials in nitrogen environment at the rate of 5 °C/min using TGA equipment. As shown in Figure 2, only 4% degradation was observed in all of the material up to 250 °C, whereas 3% weight loss can be seen up to 100 °C, which is mainly associated with the desorbed water in the porous structures of materials. As shown in the inlet of Figure 2, further 1% weight loss from 100 to 250 °C can be attributed to the removal of some unreacted organic compounds and resins. The most common feature in all of the materials was the rapid weight loss started in the range of 350−400 °C. This third weight loss step can associated with the actual decomposition of covalent organic polymers, since almost 60% of the materials were degraded in the temperature range of 300−600 °C. This clearly indicates that, these compounds have good thermal stability and can be used at temperature as high as 250 °C. Mason et al, related the initial 7% weight loss to the removal of NH_2 group in amine modified polymer of intrinsic microporosity (PIMs) however, the covalent organic polymer presented in this article possess the intrinsic functionality without any further amine impregnation, thus, these materials have shown higher thermal stability than PIM.[30] COPs (COP-H, COP-C) reported by Sun et al. and modified with palladium nanoparticles decomposed up to 60% at around 250 °C, indicating thermal in-stability[31] as compared to our COPs materials which have shown structure strengthens under similar condition. This higher thermal stability of COPs (COP-32−37) materials can be mainly associated with the strong hydrogen bonding between building block monomers and different linkers.[32]

Additionally, three connecting nodes of building block monomer, that is, tricarbonyl trichloride can be easily chained by two connecting nodes linkers, which ensure rigidity of the materials and therefore, retain the porous structure stability at temperature as high as 300 °C.[33] Importantly, thermal stability of polymers can be further extended by conjugating surface OH ion with 3,4-diace-toxycinnamic acid (DACA), however, this will hinder CO_2 adsorption.[34] Figure 3 shows the SEM micrographs of all COPs materials with the same scale of

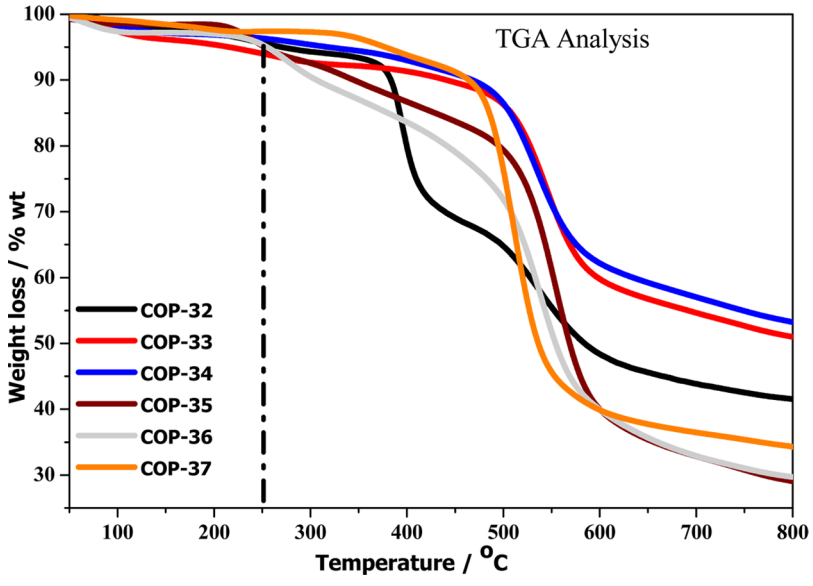

Figure 2. Thermal degradation profile of COPs-32−37 up to 800 °C, performed at 5 °C/min in N_2 atmosphere.

DOI: 10.1021/acsami.6b05927
ACS Appl. Mater. Interfaces 2016, 8, 20772−20785

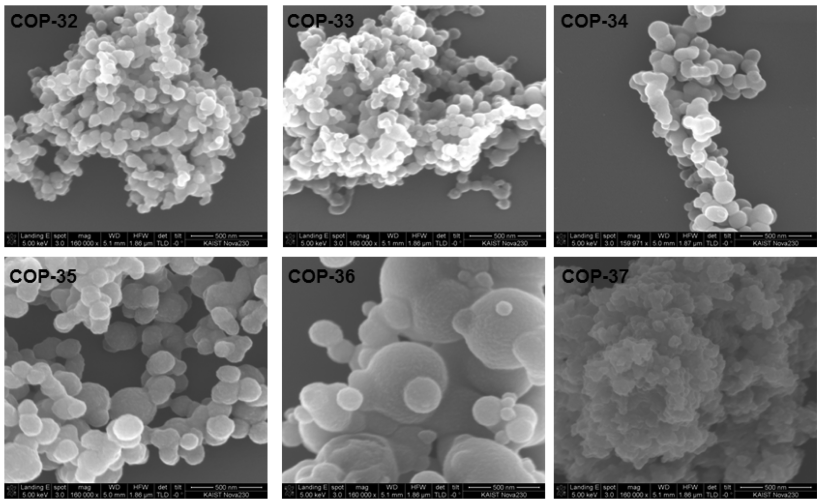

Figure 3. Morphology of COPs-32−37 obtained from FE-SEM (bar scale = 500 μm).

magnification (×100 000). It can be seen from the SEM images that COP-32−34 are in the form of agglomeration and have almost similar structures and sizes. In case of COP-32 and COP-33 very small sizes particles aggregated to form bunch like structures with negligible porosity, however, in case of COP-34 small sizes particles made elongated structures indicating formation of chain polymers.

On the other hand ester linker based COPs (COP-35−36) except for COP-37 have almost bigger size agglomerates with different sizes from very small to very large spherical like assemblies. SEM images further reveal that COP-37 has very small particle size as compared to other counterpart where the material makes a plum like shape. Although COP-35 has different sizes particulate, however, the overall size of this material is smaller than COP-36 but, larger than COP-37. Since, single building block monomer, that is, tricarbonyl trichloride has been used for the synthesis of these materials, however, variation in the aggregation of particles to form agglomerated structure can be attributed to the differences in the connecting sites of various linkers.

Along with functionality[35] and selectivity, pore volume and surface area also play crucial role[36] in adsorption−desorption performance of solid sorbents to capture large quantity of flue gases.[37] Physical parameters, such as pore volume, surface area, pore volume distribution and pore size of COPs materials were investigated through liquid nitrogen adsorption−desorption isotherms, as shown in figures given in Supporting Information (Figure S2). It is evident that N_2 isotherms of all materials have type III characteristics indicating multilayer pore filling with weak interaction between adsorbate and adsorbent.[38] Detail investigation of the pore size distribution (Figure S2), reveal that COP-32-COP-34 have both mesoporous and macro porous sizes pore diameters, while COP-35 and COP-36 are mostly mesoporous structures.

Table 2 shows the physical properties, that is, BET surface areas, pore volume, and density of COPs materials. Excluding COP-37, it can be seen that amide based polymers have generally greater surface area and larger pore volume than ester type materials. Among all the materials COP-35 has the lowest BET surface area of 5.4 m^2/g, whereas COP-37 has the largest BET surface are of 54.2 m^2/g. On the other hand COP-33 has the largest pore volume of 0.2 cm^3/g, with the second largest Langmuir surface area of 73.4 m^2/g, however, COP-36 has the smallest pore volume among all COPs materials. The surface area and pore volume of these COPs materials (COP-32−37) are found to be much smaller than the other COPs materials (COP-1−4) which was measured to be 2015 m^2/g and 1.76 cm^3/g.[39] The lower surface area and smaller pore volumes of COP-32−37 than COPs materials prepared and they can be attributed to the differences in the aromatic rings of backbone monomers.[39] COP-1−4 have been prepared with tris(4-bromophenyl) benzene, which have 3 benzene rings in the building block monomers, while COP-32−37 have a single benzene ring in the building block monomer (benzene tricarbonyltrichloride). It can be assumed that the structures of COP-34−37, which have single benzene ring in the backbone may be more compact due to the attachment of large number of linkers' molecules. However, in case of COP-1 to COP-4 backbone monomers have three benzene rings and each ring is connected by linkers making a hexagonal like loop structures with more unoccupied free space within the molecules.[39] The loop like molecular arrangements in COPs prepared previously elsewehere[39,40] allows larger space within the structure as compared to the squeezed structures of COP-32−37, which results in larger pore volume and larger surface area.

Table 2. BET Analysis and Physical Properties of COPs Materials

	material density (g/cm^3)		surface area (m^2/g)		
material	bulk	tapped	BET	Langmuir	pore volume (cm^3/g)
COP-32	0.152	0.190	46.00	63.80	0.139
COP-33	0.122	0.156	53.20	73.40	0.200
COP-34	0.194	0.253	33.40	46.20	0.095
COP-35	0.086	0.125	5.40	7.50	0.110
COP-36	0.146	0.220	11.10	15.40	0.032
COP-37	0.135	0.200	54.20	75.00	0.190

Adsorption capacity of COPs materials were first tested with BET apparatus for CO_2 and N_2 gases at standard temperature and pressure. Table 3 shows the overall performance of all the materials at low pressure of 1 bar and 298 K, which reveals that COP-33 has the highest CO_2 adsorption capacity, whereas COP-36 has the highest N_2 adsorption capacity. Adsorption isotherms of CO_2 and N_2 at 298 K and 1 bar are given in

DOI: 10.1021/acsami.6b05927
ACS Appl. Mater. Interfaces 2016, 8, 20772−20785

Table 3. CO_2 and N_2 Adsorption Capacity and Selectivity at 298 K and 1 bar

	uptake (mmol/g)		
COPs	CO_2	N_2	selectivity CO_2:N_2
COP-32	0.444	0.020	22:1
COP-33	0.600	0.019	32:1
COP-34	0.470	0.024	20:1
COP-35	0.283	0.022	13:1
COP-36	0.330	0.023	15:1
COP-37	0.444	0.0175	25:1

Supporting Information (Figure S3), which clearly demonstrate that COP-33 up takes 0.5963 mmol/g CO_2 which is the highest among all and more than twice the uptake by COP-35 (0.2831 mmol/g). Additionally, COP-33 has the best selectivity of 32:1 for CO_2:N_2 than all other materials, whereas COP-35 has the lowest overall performance as long as the adsorption capacity of materials is concern. When all materials are considered, better gas uptake performance of COP-33 among the other materials, particularly in comparison to COP-35 can mainly be attributed to the largest pore volume and high surface area. On the hand COP-35 has the smallest surface area among all materials, which makes this material less capable to adsorb CO_2 at these pressure and temperature conditions.

All COP materials were further examined for adsorption of CO_2 as well as N_2 and CH_4 at 10 bar and different temperatures. The adsorption desorption isotherms of CO_2 at 10 bar and two different temperatures, that is, 298 and 323 K are given in Figure 4, where Table 4 shows the complete experimental data, however, N_2 and CH_4 adsorption isotherms can be viewed in the Supporting Information. It is evident from Figure 4 that like ambient condition COP-33 adsorbed more CO_2 than all other COPs materials at increased pressure of 10 bar and 298 and 323 K. However, CO_2 uptake of COP-33 was 1.44 mmol/g at 298 K, which was reduced to 0.98 mmol/g at higher temperature of 323 K, due to the exothermic characteristic of adsorption process. Figure 4, further reveals that amide based polymers COP-33, COP-32, and COP-34 generally up take more CO_2 than ester based materials i.e. COP-35, COP-36, and COP-37 at same pressure and temperature conditions. It can be seen that CO_2 uptake capacity of amide type polymers (COP-32, COP-33, and COP-34) vary according to the size of their pore volume and surface area. Since, trend in the CO_2 adsorption capacity of amide based materials is COP-33 > COP-32 > COP-34, which is exactly similar to the pore volume (0.2 > 0.139 > 0.095 cm^3/g) and surface areas of these materials.

Similarly, effect of pore volume on the adsorption capacity of CO_2 at lower pressure was also observed in ester-based materials, since the pore volume and adsorption capacity were vary as COP-37 > COP-35 > COP-36 which are given in Table 2 and 3. This effect of pore volume on CO_2 uptake capacity is prominent at higher temperature of 323 K as compared to 298 K. Additionally, various researchers have correlated the adsorption capacity of materials with concentration of nitrogen functionality, however, in our case COP-34 up take lowest CO_2 among the amide based polymers though it has the largest content of nitrogen. It can be deduced from these findings that at lower pressure (up to 10 bar), pore volume, and surface areas not the N content are the main drivers for high quantity CO_2 adsorption in amide based covalent organic polymers. Xiang et al.[39] also found similar effect of pore volume on the CO_2 adsorption capacity in three covalent organic polymers (namely, COP-1, COP-2, COP-3) with the exception of COP-4, which showed highest surface area and was prepared from triazine and has N enriched structure. Upon comparing the physical parameters (such as surface area and pore volumes) and adsorption capacity of porous COP32−37 materials with literature, it can be seen that porous aromatic framework (PAF)[41] having surface area as high as 5600 m^2/g up takes 1300 mg/g (about 33 mmol/g) at 48 bar and 298 K. Similarly, PPN-4 with surface area of 6610 m^2/g and pore volume of 3.04 cm^3/g, adsorbs 50 mmol/g CO_2 at 50 bar and 295 K.[42]

Upon checking the adsorption capacity of these materials for N_2 and CH_4 it can be seen that COP-33 and COP-34 adsorb certain quantities of gases other than CO_2 at pressure of 10 bar, however, all other materials are almost inert and do not uptake other N_2 and CH_4. As shown in Table 4 COP-33 adsorb comparatively more nitrogen and methane than all other materials, which are 0.61 and 0.41 mmol/g at 298 K and 10 bar. As a general analysis it can be assume that amide based COPs materials adsorb certain amount of N_2 and CH_4 along with CO_2; however, ester-based materials are totally inactive for adsorption of N_2 and CH_4 at pressure up to 10 bar and temperatures of 298 and 323 K.

Since, pore volume and surface areas of amide based COPs are higher than the ester based materials, preliminary, it can be assumed that these physical properties are responsible for adsorption of N_2 and CH_4 by amide type COPs materials. Additionally, selectivity of most of the ester-based polymers (COP-36, COP-37) is much higher than that of amides COPs

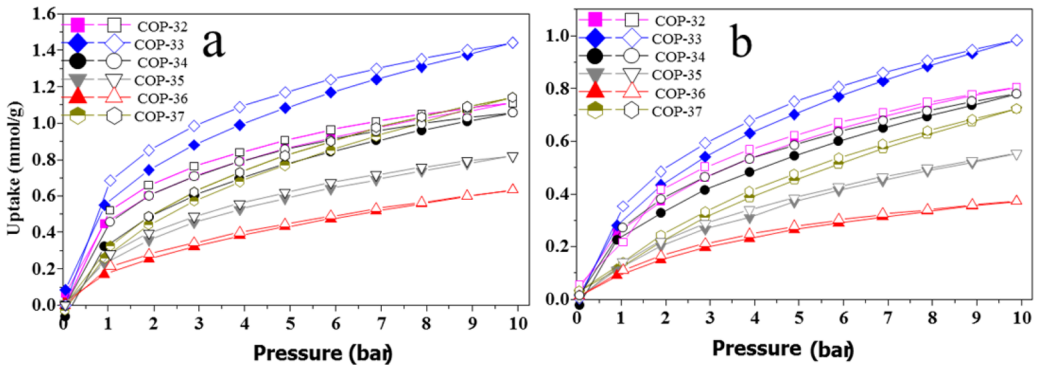

Figure 4. CO_2 adsorption at (a) 298 and (b) 323 K and 10 bar.

DOI: 10.1021/acsami.6b05927
ACS Appl. Mater. Interfaces 2016, 8, 20772−20785

Table 4. Maximum Adsorption of N_2, CO_2, and CH_4 by COP Materials at 10 bar

	CO_2 (mmol/g)		CH_4 (mmol/g)		N_2 (mmol/g)		selectivity (CO_2:N_2:CH_4)	
	temperature							
material	298 K	323 K	298 K	323 K	298 K	323 K	298 K	323 K
COP-32	1.11	0.80	0.22	0.08	0.08	0.04	14:1:3	20:1:2
COP-33	1.44	0.98	0.41	0.29	0.61	0.26	4:1:2	4:1:1
COP-34	1.12	0.78	0.41	0.19	0.18	0.06	6:1:2	14:1:3
COP-35	0.82	0.55	0.18	0.13	0.08	0.06	10:1:3	9:1:2
COP-36	0.56	0.37	0.07	0.02	0	0	∞	∞
COP-37	1.14	0.72	0.19	0.11	0.21	0	∞	∞

(COP-32, COP-33, and COP-33). Among amide type COPs materials, COP-32 has better selectivity, than COP-33 and COP-34 at 323 K and 10 bar, however, selectivity of COP-33 is better than all other materials at 298 K and 10 bar. It must be noted that, COP-33 has also best selectivity among all other materials for CO_2 over N_2 at 298 K and 1 bar. Figure 5 reveals

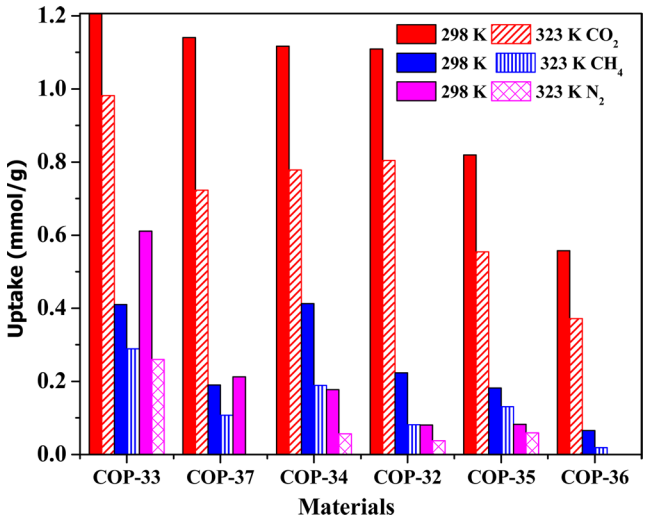

Figure 5. Overall performance of all COPs (32−37) materials showing maximum adsorbed capacity of CO_2, CH_4, and N_2 at 10 bar and 298 and 323 K.

that with the exception of small differences, COP-33, COP-37, COP-34, and COP-32 almost uptake similar CO_2 adsorption quantity at 10 bar and room temperature, whereas, COP-35 and COP-36 adsorb lower amount of CO_2 under similar condition. The lower CO_2 adsorption at these pressure and temperature conditions by COP-35 and COP-36 can be associated with the lower pore volume and lower surface area as compared to other COPs materials presented in this article.

Precombustion such as in integrated gasification combine cycle system (IGCC) requires CO_2 separation and capture and relatively high pressure and high temperature, thus COPs materials were also tested under high pressure and high temperature.[43] Performance of all the materials at high pressure up to 200 bar for CO_2 uptake is shown in Figure 6, where the isotherms were obtained at three different temperatures of 308, 323, and 338 K. Detail investigation of adsorption/desorption isotherms reveal that behavior of adsorption before the critical pressure range (70−80 bar) is different than that above this pressure value. It is evident that at low pressure, that is, up to the maximum of 80 bar adsorption is gradually increasing with pressure similar to type III isotherms, which represents very weak adsorbate−adsorbent interaction unlike to type II and IV isotherms which have a knee in this range indicating monolayer formation. This particular behavior of the isotherms at this pressure range has been associated with the localized adsorption of CO_2 molecules in the vicinity of the unfilled pores.[44] Upon comparing the adsorption isotherms of COP materials in the present study to that of polymers of intrinsic microporosity (PIMs) investigated by Regno et al.[45] it can be seen that unlike to our case, there is a sharp increase in the adsorption of CO_2 at the lower pressure range which was mainly attributed to the microporosity of materials. However, in our case after the critical pressure range a sharp rise in the adsorption is observed with increase in pressure which is extended up to the pressure of 130 bar, whereas at further high pressure the CO_2 up take was almost flat with pressure and the isotherms have very low slope in this region. Here, in we argue that at above critical pressure (around 71 bar), both pore fillings and enhancement in the interaction of adsorbate−adsorbent commenced resulting in abrupt increase in the CO_2 up take, which leads to the formation of type V isotherms without hysteresis.

As shown in Figure 6 CO_2 isotherms of all the materials have similar trend of large adsorption at low temperature, that is, the adsorption capacity varies with temperature as 308 > 323 and 338 K; however, in case of COP-37, the adsorption isotherms were a bit different at low pressure values. COP-37 has lower adsorption capacity at lower pressure and lower temperature, which is contrary to all other materials. Nevertheless, the trend of isotherms in COP-37 returns back to the established conditions (i.e., higher adsorption at lower temperatures) only at high pressure. This unusual behavior of COP-37 for CO_2 adsorption at the lower pressure range may be associated with the difference in the surface of this material, since COP-37 has different surface texture than all other COPs materials as can be noticed in the SEM images. Figure 6 further reveals that among the amide base materials, COP-34 has the lowest CO_2 capacity whereas COP-32 and COP-33 has almost similar performance with a small increase of capacity in case of COP-33. On the other hand among the ester based materials, COP-36 has the lowest CO_2 capturing capacity, while COP-35 has the largest adsorption capability, which is opposite to the performance of these materials at 1 bar and room temperature.

CO_2 up take of all materials at 308 K and 200 bar has been compared in Figure 7, which reveals that adsorption capacity varies as COP-35 > COP-33 > COP-32 > COP-37 > COP-36 > COP-34. It must be noted COP-32 and COP-33 has almost similar performance at 308 K followed by COP-37, however, COP-36 and COP-34 fall in the same category with lowest adsorption under similar condition. Upon matching the physical properties of these compounds with adsorption capacity at 308 K and high pressure of 200 bar, it can be deduce that surface areas and pore volumes are not the driving

DOI: 10.1021/acsami.6b05927
ACS Appl. Mater. Interfaces 2016, 8, 20772−20785

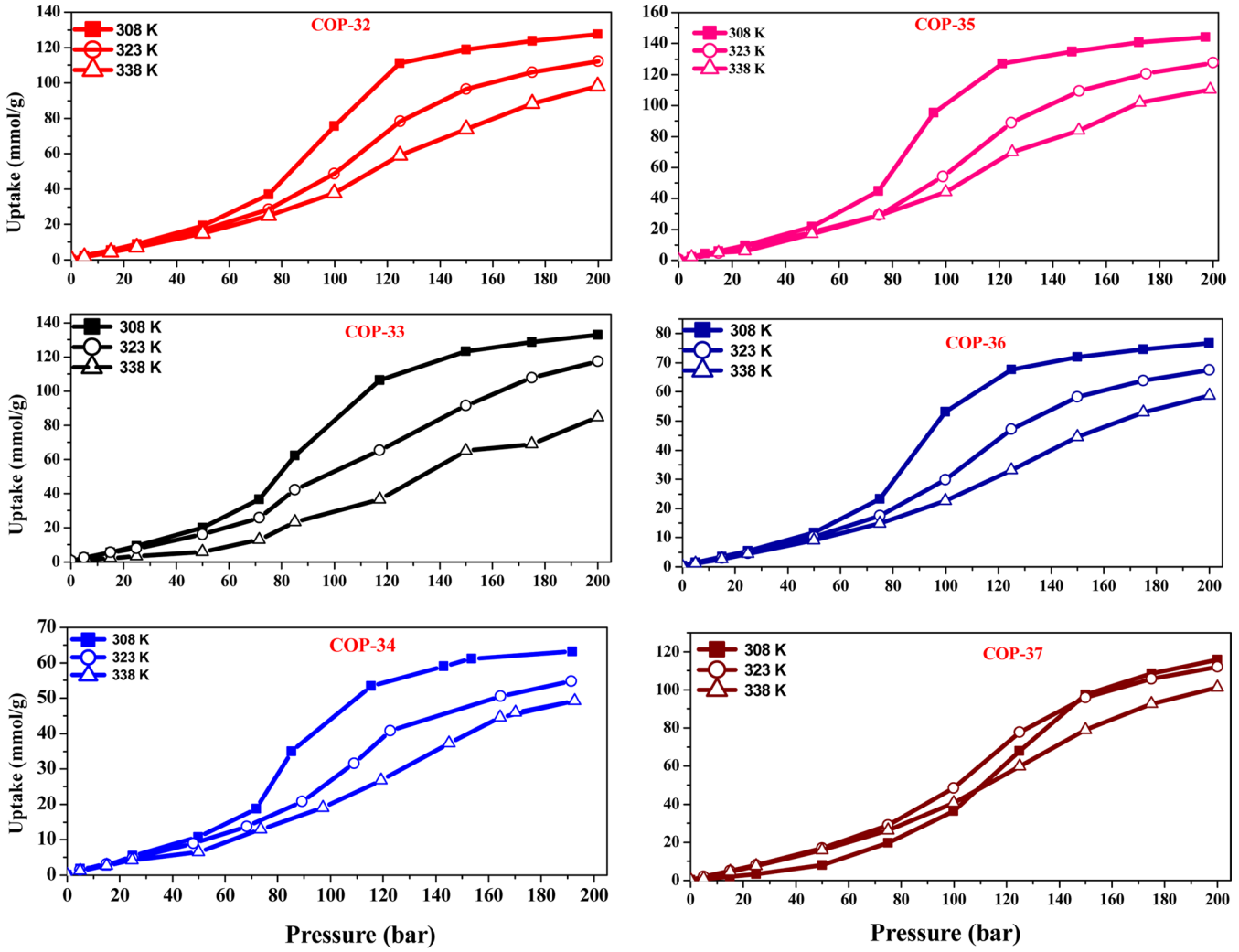

Figure 6. CO_2 uptake by all COPs (32−37) at 200 bar and 308, 323, and 338 K.

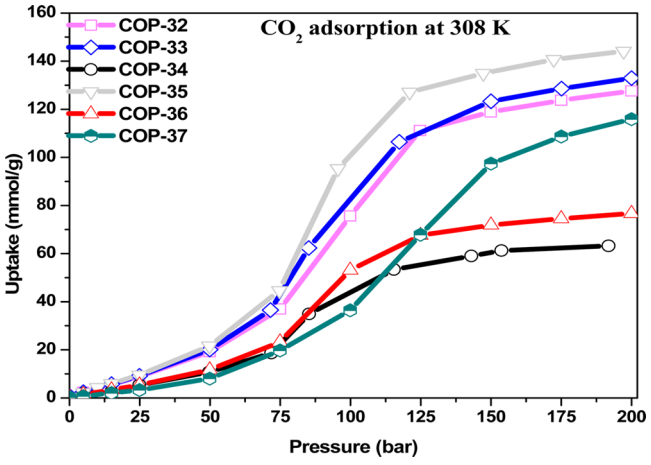

Figure 7. CO_2 uptake by all COPs materials at 308 K and 200 bar.

forces for the maximum adsorption of COPs materials, since COP-35 has the lowest surface area of 5.4 cm^3/g but has the largest capacity among all other materials. Similarly, Montagnaro et al.[46] has recently compared the CO_2 adsorption of two different activated carbon samples and showed that compound with lower pore volume has larger CO_2 adsorption capacity than that which has almost double pore volume. As stated earlier, at lower pressure and lower temperature, physical properties of the materials may have influence on the adsorption capacities of these covalent organic polymers, however, at high pressure and high temperatures, CO_2 affinity, active sites electrostatic interaction with adsorbate molecule and effect of pressure and temperature on the polarity of adsorbate and adsorbent, and on the physical properties (surface and pore volume) of materials may contribute to the enhanced CO_2 adsorption.[47]

Similarly, nature and texture properties variations of COPs materials may also play important role in the adsorption capacity, since the surface functionality of ester-based materials (COP-35−37) are different than the amide based materials and will behave differently to the environmental condition of pressure and temperature which lead to the largest adsorption in case of COP-35 as compared to other counterparts.[46] Main reason for the CO_2 adsorption on the solid sorbent is the active sites such as as $-NH_2$, −OH, −N, defect sites and electrostatic environment that surround these sites which leads to stronger interactions with surrounding CO_2 environment around the specimen that is being tested. Additionally, variation in the adsorption mode and interaction of CO_2 with different sites are different in case of amide and ester based materials and will definitely impact the adsorption capacity of these compounds at high pressure and high temperature.[48] In case of amide-based

DOI: 10.1021/acsami.6b05927
ACS Appl. Mater. Interfaces 2016, 8, 20772−20785

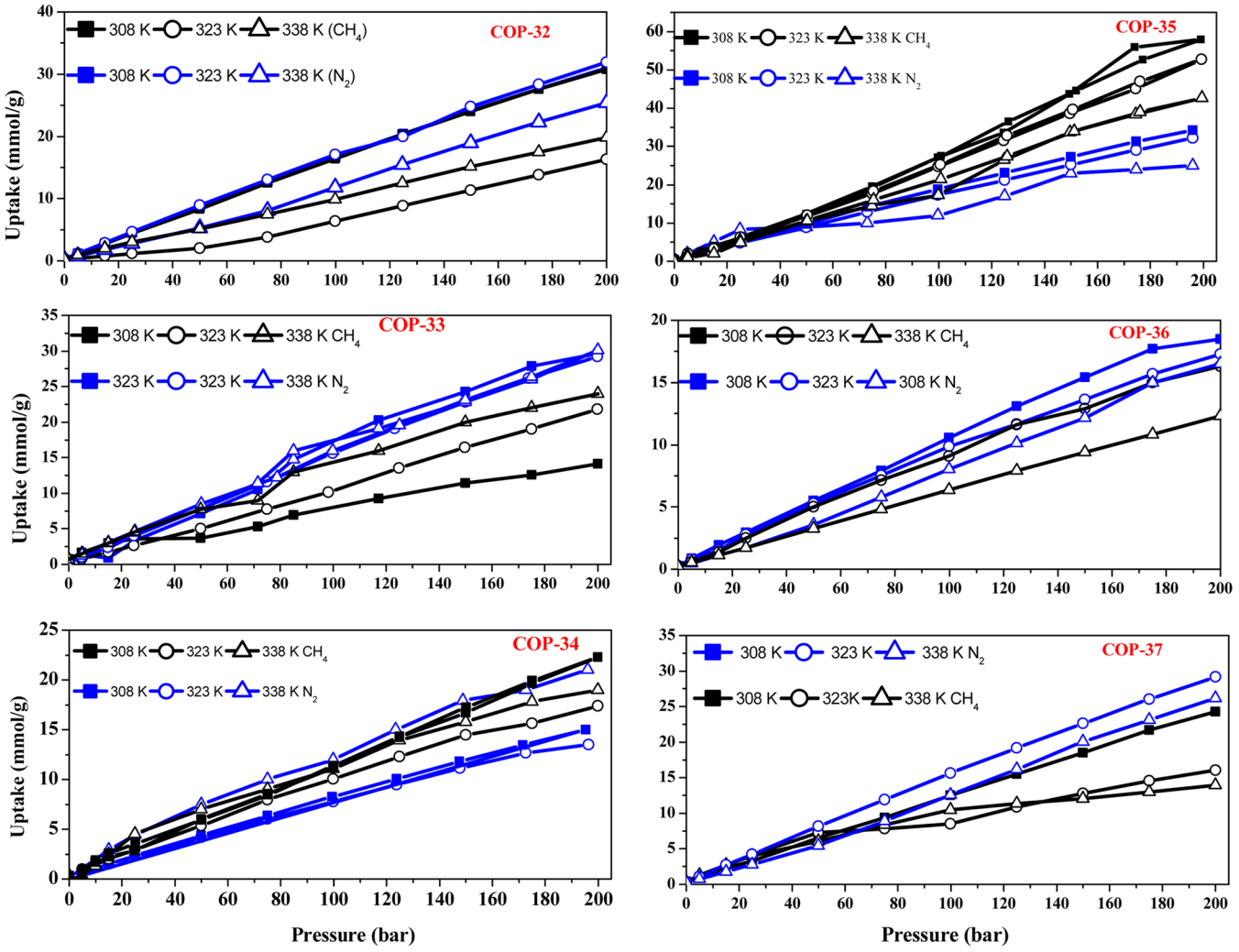

Figure 8. CH_4 and N_2 uptake by all COPs (32−37) at 200 bar and 308, 323, and 338 K.

material (COP-32−34), nitrogen functionality is mainly responsible for CO_2 adsorption which plays important role at lower pressure and temperature; however, in case of ester-based materials (COP-35−37) hydroxyl ion is the main function group on the surface of materials which can coordinate with CO_2 molecule more effectively as compared to the N functionality at high pressure.[48] Here in we assume that, at high pressure the defects sites on COP-35 surface become more favorable for CO_2 molecules due to the enhancement in the strength of coulomb forces and Van der Waal forces resulting in increased adsorption capacity.[49] Additionally, although COP-35 has the lowest surface area and less pore volume than other materials, however, it may have more defect sites containing OH ion on these sites which effectively capture CO_2 with the support of mainly hydrogen bonding as evident in the literature.[48] Liu et al.[50] have predicted that oxygen containing functional group associated with the defect sites on the surface of solid adsorbents enhances adsorption of CO_2 leading to the increased adsorption capacity. We therefore believe that COP-35 has more defect sites with associated oxygen function group as discussed in the literature[51] which interact with the available adsorbate (CO_2) molecules more effectively at high pressure, thus leading to increased CO_2 adsorption capacity.

All the materials were also tested for other gases, that is, CH_4 and N_2 at high pressure of 200 bar and three different temperatures to get the complete scenario of the materials behavior for adsorption of CO_2 as well as other gases. Figure 8 compares the isotherms of CH_4 and N_2 of each material at three different temperatures and pressure of 200 bar, which reveal that COP-32 and COP-34 almost adsorb similar quantities of CH_4 and N_2, while COP-33 uptake more N_2 than CH_4 under similar condition of pressure and temperature. Additionally, ester based materials (COP-36 and COP-37) adsorb N_2 more effectively than CH_4, whereas COP-35 up take larger quantity of CH_4 than N_2 under similar pressure and temperature conditions. Detail discussion on the CH_4 and N_2 adsorption mechanism and behavior of COPs materials is out of the scope of the present study, however, the adsorption data was obtained in order to check the material interaction with gases other than CO_2.

H_2 adsorption capacities were measured in order to examine the expected application of these materials in precombustion capture and separation systems. All materials were subjected to same pressure of 200 bar at sing temperature of 308 K to compare their H_2 uptake capacity with CO_2 adsorption capacity at similar conditions. Adsorption isotherms given in Figure 9 shows that COP-35 which has the largest CO_2 capacity (144 mmol/g) can captures only 13 mmol/g of H_2 at high pressure

DOI: 10.1021/acsami.6b05927
ACS Appl. Mater. Interfaces 2016, 8, 20772−20785

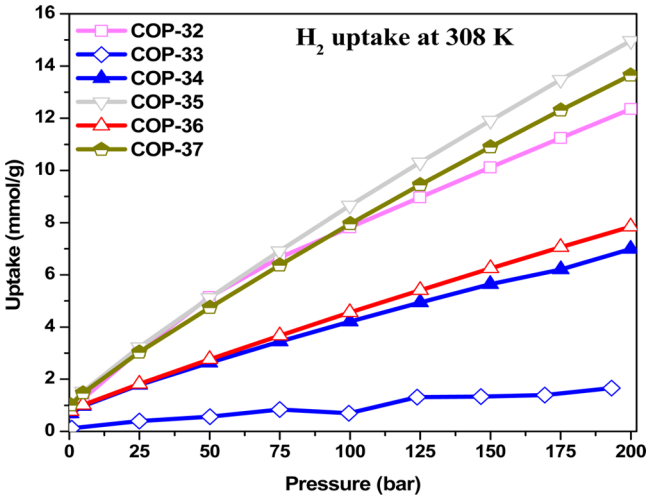

Figure 9. H_2 adsorption data for all COPs materials at 200 bar and 308 K.

of 200 bar and 308 K. On the other hand COP-33 adsorbed significantly less quantity of H_2 (1.7 mmol/g) as compared to other counterparts and hence the selectivity of this material is 78 for CO_2/H_2, which is the highest among all COPs materials.

Figure 10 and Table 5 show the data and overall performance of all COPs materials at three different temperatures (308, 323,

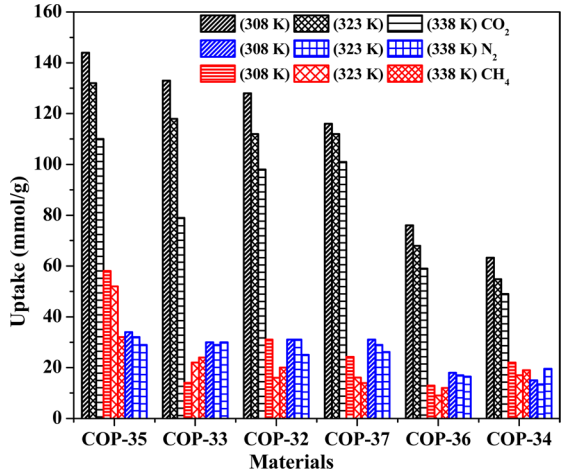

Figure 10. Overall performance of all materials for CO_2, CH_4, and N_2 adsorption at 200 bar and three different temperatures.

Table 5. Maximum Adsorption of N_2, CO_2, and CH_4 by COP Materials at 200 bar

	CO_2 (mmol/g)			CH_4 (mmol/g)			N_2 (mmol/g)		
	temperature (K)								
material	308	323	338	308	323	338	308	323	338
COP-32	128	112	98	31	16	20	31	31	25
COP-33	133	118	79	14	22	24	30	29	30
COP-34	63	55	49	22	17	19	15	14	20
COP-35	144	128	110	58	52	42	34	32	29
COP-36	76	68	59	18	16	12	18	17	16.5
COP-37	116	112	101	24	16	14	31	29	26

and 338 K) for the maximum adsorption of CO_2, CH_4, and N_2 at 200 bar. It is evident from Figure 10 and Table 5 that COP-35 uptakes the maximum CO_2 quantity of about 144 mmol/g at 308 K which is known to be the largest capturing capacity of solid sorbent, recorded for the first time in the literature under similar condition. However, owing to the exothermic effect of the adsorption process CO_2 up take was reduced to 128 and 110 mmol/g at higher temperature of 323 and 33 K. Upon comparing the capturing capacity of materials at 308 K and 200 bar, it can be seen that maximum adsorption capacity for CO_2 varies as COP-35 > COP-33 > COP-32 > COP-37 > COP-36 > COP-34, which is irrelative to the physical properties such as pore volume and surface areas of materials. Figure 10 and Table 5 also represent the adsorption capacities of these materials under similar condition for CH_4 and N_2, it can be seen that with a minute difference all the materials almost behave similarly for gases other than CO_2. However, at low pressure this trend of CH_4 and N_2 adsorption was different than that at high pressure, since at low pressure of 10 bar, COP-36 and COP-37 even could not up take any N_2 giving rise very high selectivity for CO_2/N_2.

Selectivity of COPs materials at high pressure of 200 bar and three different temperatures given in Table 6 indicates that

Table 6. Selectivity of COP Materials at 200 bar

	temperature (K)		
	308	323	338
material	CO_2:CH_4:N	CO_2:CH_4:N	CO_2:CH_4:N_2
COP-32	4:1:1	7:1:2	5:1:1
COP-33	10:1:2	5:1:1	4:1:2
COP-34	4:1:1	4:1:1	3:1:1
COP-35	4:2:1	4:2:1	4:2:1
COP-36	6:1:1	7:1:2	5:1:1
COP-37	5:1:1	7:1:2	7:1:2

along with the highest adsorption capacity COP-35 also have best selectivity among all other materials. Selectivity was calculated based on single gas sorption data collection at a time getting the normalized sorption data among the gas sorption values. As shown in Table 6 selectivity of COP-33 for CO_2:CH_4:N_2 is 10:1:2 at 308 K which is highest among all other followed by COP-36 with the selectivity of 6:1:1 at 308. It must also be noted that selectivity of COP-35 is almost comparable to COP-34 where both are about stable at all other temperatures of 323 and 338 K whereas selectivity of COP-33 reduced to 5:1:1 and 4:1:2 under similar conditions. It is important to note that although, COP-35 has comparatively similar selectivity to COP-34 however, the former has the highest adsorption capacity whereas the later has the lowest adsorption capacity.

Since adsorption is exothermic process and lot of heat is liberated when adsorption take place on the adsorbent surface,[52] we therefore calculate the heat of adsorption (shown in Figure 11) for each material at 308 K using Clapeyron equation at particular number moles of CO_2 captured by the adsorbents.[53] As shown in Figure 11, the material with largest adsorption quantity has highest heat of adsorption, which is decreasing rapidly with increasing the number of adsorbed mole on the materials surfaces. COP-35 has the highest heat of adsorption followed by COP-33, COP-32 and COP-37, which is similar to the adsorption trend of CO_2 (Figure 7). Additionally, COP-34 and COP-36 have the lowest adsorption as well as lowest heat of adsorption, which

DOI: 10.1021/acsami.6b05927
ACS Appl. Mater. Interfaces 2016, 8, 20772−20785

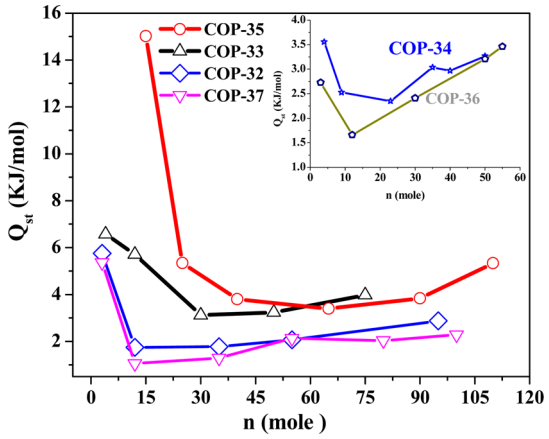

Figure 11. Heat of adsorption associated with CO_2 adsorption at 308 K.

represent the lower performance of these two materials for CO_2 up take.

A detailed investigation of Figure 11 indicates that for all materials isosteric heat of adsorption initially decreasing immediately form the largest value, become flatten and then increases a little bit as the adsorbed number of moles increases. Krungleviciute et al.[54] also observed almost similar trend in the isosteric heat of adsorption for the carbon nanotube, where increase in the heat of adsorption at high surface coverage was attributed to the intrainteraction of adsorbate molecules on the surface.

Although, COP-35 has 15.01 kJ/mol heat of adsorption which is the largest among all other COPs materials, however, this is much lower than that of other physical adsorbents such as polymers (20.3 kJ/mol),[55] metal organic frame-works (90 kJ/mol),[56] zeolites (50 kJ/mol),[57] and functionalized silica (100 kJ/mol). Riech et al.[58] found that a nanoporous borazine-linked polymer (BLP-1) has 22.2 kJ/mol heat of adsorption which is least among all other materials for CO_2 however, this material has very low selectivity for CO_2 over methane. It is evident that, COPs material possesses very low heat of adsorption, which makes these compounds more favorable as long as regeneration and repeated use of the adsorbents are concern.

As an essential property of adsorption−desorption process, rate of adsorption was calculated via mathematical expression mentioned in literature[59] in the term of mass transfer coefficient k (1/sec) (shown in Figure 12) at two different temperatures and pressure of 10 bar from the adsorbed quantity of CO_2 at particular pressure values. It is important to note that although COP-33 comparatively adsorbed more CO_2 at 10 bar, however, its rate of adsorption is significantly slower than all other materials. Additionally, Figure 12 further reveals that at 298 K COP-37 up take CO_2 with the fastest rate of about 0.94/sec followed by COP-33 and COP-34, whereas COP-35 and COP-36 have almost similar adsorption rate starting at around 0.5/sec. Figure 12 further indicates that in general rate of adsorption reduces for all the materials with the increase of temperature, however, in case of COP-32 temperature has negligible effect on mass transfer co efficient. Unlike to Brownian motion of gases, reduction in the rate of adsorption on the adsorbent surfaces and within the pore at high temperature is obviously due the exothermic effect of adsorption, which hinders both the adsorption capacity and moment of adsorbate on the surfaces. Since, mass transfer coefficient of CO_2 in ammonia absorption is restricted by the gas−liquid interface and the different environmental condition surrounding the gas molecules in aqueous ammonia,[60] similarly, the moment of CO_2 on solid surfaces and inside the pore is also restricted by hydrogen bonding and Van der Waal forces between adsorbate and adsorbent. Additionally, surface heterogeneity also plays important role in the adsorption process which may subsequently leads to the enhancement in heat of adsorption, as well as to the reduction in the rate of adsorption. Boa et al. noted that all gases including CO_2 and methane adsorbed quickly and the equilibrium achieves rapidly with increase in temperature using metal organic frameworks as sorbent, however, in our case as shown in Figure 12, CO_2 adsorption becomes slower with increase in temperature.[61]

In situ FTIR analysis was conducted using COP-35 as solid sorbent to ensure the interaction of CO_2 molecules with attractive sites. In a typical procedure KBr powder and COP-35 were mixed with proper ratio and then dehydrated for at least 12 h to completely remove water content form the mixture. Initially, background spectrum of only KBr pellet under vacuum was collected in order to obtain pure spectrum of only CO_2 and COP-35. It is important to note that only single peak at 2337.5 cm^{-1} is observed upon injecting CO_2 at room temperature as shown in Figure 13, which is assigned to the residual gaseous CO_2 in the atmosphere of the sample and detector compartments which could not be resolved by purging. The peak at 2337.5 cm^{-1} grows as CO_2 pressure increases, overriding the infrared absorbance of gaseous CO_2 peak at 2349 cm^{-1} until

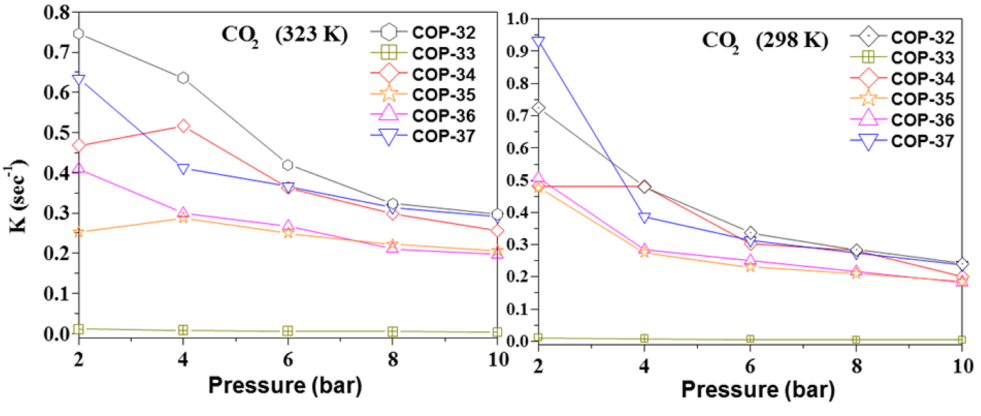

Figure 12. Rate of adsorption calculated from data of CO_2 adsorption at 298 K, 323 K, and 10 bar.

DOI: 10.1021/acsami.6b05927
ACS Appl. Mater. Interfaces 2016, 8, 20772−20785

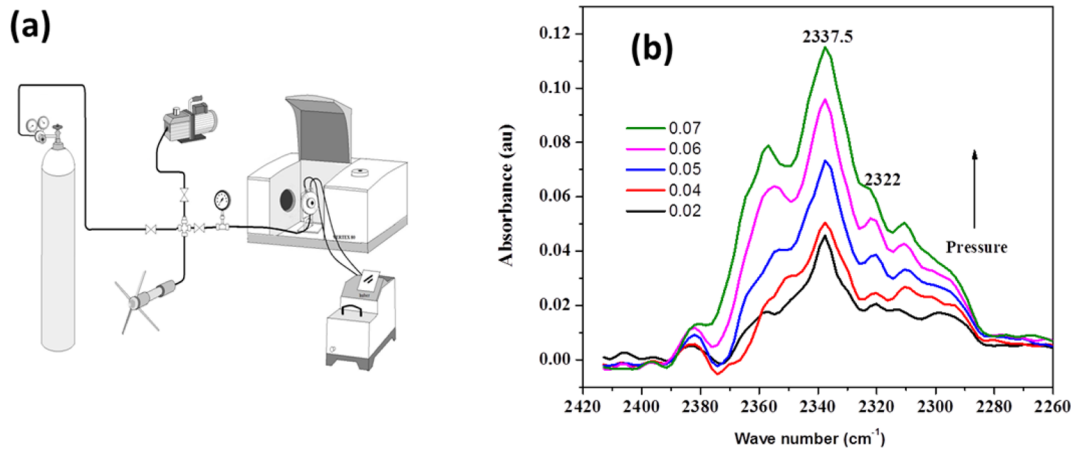

Figure 13. In situ FTIR (a) set up and (b) analysis of CO_2 adsorption by COP-35 at various pressure ranges.

the former prevails at 0.07 bar. This heterogeneous interaction is allowed for six to 8 min to ensure saturation at each pressure. The peak at 2337.5 cm^{-1} is assigned to CO_2 asymmetric stretch mode that is red-shifted with respect to the peak of gaseous CO_2, providing an evidence for the presence of at least one type of sorption sites which is responsible for CO_2 uptake by COP-35. As the pressure increases, the absorbance of infrared photons increases which indicates that CO_2 adsorbed quantity increases along with pressure. It is important to note that vibrational frequency of asymmetric stretching mode of adsorbed CO_2 on graphene surface[62] was observed at 2393 cm^{-1}, while it was detected at 2319 cm^{-1}on graphite nanoparticles.[63] Contrary, in situ FTIR analysis of yttria-stabilized ZrO_2, Y_2O_3, and pristine ZrO_2 showed that most of the adsorbed CO_2 has been chemically bonded to form various carbonate species via chemisorption process due the presence of hydroxyl group on the surfaces.[64] In our case no evidence of chemisorption was detected which indicates that COP-35 uptake CO_2 only through physical adsorption, that is, via Vander Waal interaction and columbic interaction and could be a suitable material for further investigation.

4. CONCLUSION

Six different types of covalent organic polymers (COPs) with two different functionalities, that is, OH group and N_2 based on different linkers and single building block monomers have been successfully prepared and were tested for adsorption of CO_2, CH_4, and N_2 at various temperatures and pressures. Results showed that at atmospheric condition (1 bar and 298 K) CO_2 adsorption capacities of materials were mostly dependent on the physical parameters i.e. surface areas and pores volume of these materials, therefore, COP-33 uptakes more CO_2 than other COPs materials. On the other hand COP-35 has the smallest surface area among all materials, which makes this material less capable to adsorb CO_2 at these pressure and temperature conditions. Results further revealed that at pressure of 10 bar, CO_2 adsorption capacities of amides (COP-32, COP-33, and COP-34) are strongly related to their pores volume and surface areas, since, CO_2 adsorption capacities of amides have similar trend to that of the pore volume (0.2 > 0.139 > 0.095 cm^3/g) and surface areas. It was also noticed that amides also adsorb certain quantity of N_2 and CH_4 in addition to CO_2, however, ester based materials are totally inactive for N_2 and CH_4 at 10 bar and temperatures of 298 and 323 K. Unlike to lower pressure, performances of ester materials (COP-35, COP-36, and COP-37) were different than amide type materials at high pressure of 200 bar. Interestingly, although COP-35 has the lowest surface area among all materials, however, it up take 144 mmol/g CO_2 at 308 K and 200 bar, which is the largest quantity adsorbed by any solid sorbent so far in the literature. The largest adsorption capacity of COP-35 than any other materials can be attributed to the presence of defects sites on the surface, making this material more favorable for CO_2 molecules adsorption because of the enhancement in the strength of coulomb and van der Waals forces at high-pressure valves. Since, COP-35 adsorb largest quantity of CO_2, therefore, it has the largest heat of adsorption (15 kJ/mol) among all COPs materials, but less than any other solid sorbent reported in the literature. In addition to the quantitative investigations, kinetics measurement of CO_2 adsorption conducted at 10 bar and two different temperatures revealed that COP-37 has the best while COP-33 has the lowest rate of adsorption than all other materials. COPs materials were also. On the other hand COP-33 has the best selectivity for CO_2:CH_4:N_2, which is 10:1:2 at 308 K and 200 bar, however, at atmospheric condition this material has much higher selectivity of 32:1 for CO_2:N_2. It can be deduced from the presented findings that, COP-33 has the best performance at atmospheric condition and lower pressure; however, COP-35 has shown very interesting results at high pressure of 200 bar by adsorbing the largest quantity of CO_2 so far. On the basis of these findings, it can be suggested that COP-35 needs to be further investigated at various pressure and temperature conditions including pressure swing adsorption and humidity effect on the adsorption capacity.

■ ASSOCIATED CONTENT

Supporting Information

The Supporting Information is available free of charge on the ACS Publications website at DOI: 10.1021/acsami.6b05927.

Detailed synthesis of the presented COP materials, characterization data for FTIR and BET measurements, and selectivity data based on single gas adsorption (PDF)

■ AUTHOR INFORMATION

Corresponding Authors

*E-mail: mert.atilhan@qu.edu.qa.
*E-mail: yavuz@kaist.ac.kr.

DOI: 10.1021/acsami.6b05927
ACS Appl. Mater. Interfaces 2016, 8, 20772−20785

Author Contributions

[#]Equal contribution.

Notes

The authors declare no competing financial interest.

■ ACKNOWLEDGMENTS

This paper was made possible by the support of Qatar National Research Fund, National Priorities Research Program grant (NPRP 5-499-1-088). The statements made herein are solely the responsibility of the authors.

■ REFERENCES

(1) Barandica, J. M.; Delgado, J. A.; Berzosa, Á.; Fernández-Sánchez, G.; Serrano, J. M.; Zorrilla, J. M. Estimation of CO2 emissions in the life cycle of roads through the disruption and restoration of environmental systems. *Ecological Engineering* **2014**, *71*, 154−164.

(2) Berger, A. H.; Bhown, A. S. Selection of Optimal Solid Sorbents for CO2 Capture Based on Gas Phase CO2 composition. *Energy Procedia* **2014**, *63* (0), 2092−2099.

(3) Liu, X.; Zhang, Y.; Li, H.; A, S.; Xia, H.; Mu, Y. Triarylboron-based fluorescent conjugated microporous polymers. *RSC Adv.* **2013**, *3* (44), 21267−21270.

(4) Ullah, R.; Atilhan, M.; Diab, A.; Deniz, E.; Aparicio, S.; Yavuz, C. T. Synthesis, characterization and evaluation of porous polybenzimidazole materials for CO2 adsorption at high pressures. *Adsorption* **2016**, *22*, 247−260.

(5) Belmabkhout, Y.; Guillerm, V.; Eddaoudi, M. Low concentration CO2 capture using physical adsorbents: Are metal−organic frameworks becoming the new benchmark materials? *Chem. Eng. J.* **2016**, *296*, 386−397.

(6) Prudencio, A.; Schmeltzer, R. C.; Uhrich, K. E. Effect of Linker Structure on Salicylic Acid-Derived Poly(anhydride−esters). *Macromolecules* **2005**, *38* (16), 6895−6901.

(7) Liu, G.; Wang, Y.; Shen, C.; Ju, Z.; Yuan, D. A facile synthesis of microporous organic polymers for efficient gas storage and separation. *J. Mater. Chem. A* **2015**, *3*, 3051−3058.

(8) Patel, H. A.; Ko, D.; Yavuz, C. T. Nanoporous Benzoxazole Networks by Silylated Monomers, Their Exceptional Thermal Stability, and Carbon Dioxide Capture Capacity. *Chem. Mater.* **2014**, *26*, 6729−6733.

(9) Patel, H. A.; Karadas, F.; Canlier, A.; Park, J.; Deniz, E.; Jung, Y.; Atilhan, M.; Yavuz, C. T. High capacity carbon dioxide adsorption by inexpensive covalent organic polymers. *J. Mater. Chem.* **2012**, *22* (17), 8431−8437.

(10) Liebl, M. R.; Senker, J. Microporous Functionalized Triazine-Based Polyimides with High CO2 Capture Capacity. *Chem. Mater.* **2013**, *25* (6), 970−980.

(11) El-Kaderi, H. M.; Hunt, J. R.; Mendoza-Cortés, J. L.; Côté, A. P.; Taylor, R. E.; O'Keeffe, M.; Yaghi, O. M. Designed Synthesis of 3D Covalent Organic Frameworks. *Science* **2007**, *316* (5822), 268−272.

(12) McKeown, N. B.; Budd, P. M. Polymers of intrinsic microporosity (PIMs): organic materials for membrane separations, heterogeneous catalysis and hydrogen storage. *Chem. Soc. Rev.* **2006**, *35* (8), 675−683.

(13) Sekizkardes, A. K.; Islamoglu, T.; Kahveci, Z.; El-Kaderi, H. M. Application of pyrene-derived benzimidazole-linked polymers to CO2 separation under pressure and vacuum swing adsorption settings. *J. Mater. Chem. A* **2014**, *2* (31), 12492−12500.

(14) Xiao, Q.; Liu, Y.; Zhong, Y.; Zhu, W. A citrate sol-gel method to synthesize Li2ZrO3 nanocrystals with improved CO2 capture properties. *J. Mater. Chem.* **2011**, *21* (11), 3838−3842.

(15) Kato, M.; Nakagawa, K.; Essaki, K.; Maezawa, Y.; Takeda, S.; Kogo, R.; Hagiwara, Y. Novel CO2 Absorbents Using Lithium-Containing Oxide. *Int. J. Appl. Ceram. Technol.* **2005**, *2* (6), 467−475.

(16) Zhang, X.; Long, E.; Li, Y.; Guo, J.; Zhang, L.; Gong, M.; Wang, M.; Chen, Y. CeO2-ZrO2-La2O3-Al2O3 composite oxide and its supported palladium catalyst for the treatment of exhaust of natural gas engined vehicles. *J. Nat. Gas Chem.* **2009**, *18* (2), 139−144.

(17) Bai, R.; Yang, M.; Hu, G.; Xu, L.; Hu, X.; Li, Z.; Wang, S.; Dai, W.; Fan, M. A new nanoporous nitrogen-doped highly-efficient carbonaceous CO2 sorbent synthesized with inexpensive urea and petroleum coke. *Carbon* **2015**, *81* (0), 465−473.

(18) Wu, Z.; Webley, P. A.; Zhao, D. Post-enrichment of nitrogen in soft-templated ordered mesoporous carbon materials for highly efficient phenol removal and CO2 capture. *J. Mater. Chem.* **2012**, *22* (22), 11379−11389.

(19) Xing, W.; Liu, C.; Zhou, Z.; Zhou, J.; Wang, G.; Zhuo, S.; Xue, Q.; Song, L.; Yan, Z. Oxygen-containing functional group-facilitated CO(2) capture by carbide-derived carbons. *Nanoscale Res. Lett.* **2014**, *9* (1), 189−189.

(20) Sánchez-Sánchez, Á.; Suárez-García, F.; Martínez-Alonso, A.; Tascón, J. M. D. Influence of Porous Texture and Surface Chemistry on the CO2 Adsorption Capacity of Porous Carbons: Acidic and Basic Site Interactions. *ACS Appl. Mater. Interfaces* **2014**, *6* (23), 21237−21247.

(21) Zulfiqar, S.; Sarwar, M. I. Probing the potential of polyester for CO2 capture. *J. Environ. Sci.* **2014**, *26* (7), 1423−1427.

(22) Karadas, F.; Yavuz, C. T.; Zulfiqar, S.; Aparicio, S.; Stucky, G. D.; Atilhan, M. CO2 Adsorption Studies on Hydroxy Metal Carbonates M(CO3)x(OH)y (M = Zn, Zn−Mg, Mg, Mg−Cu, Cu, Ni, and Pb) at High Pressures up to 175 bar. *Langmuir* **2011**, *27* (17), 10642−10647.

(23) Lemmon, E. W., Huber, M. L., McLinden, M. O. *NIST Standard Reference Database 23: Reference Fluid Thermodynamic and Transport Properties-REFPROP*, version 9.1; National Institute of Standards and Technology, Standard Reference Data Program: Gaithersburg, MD, 2013.

(24) Mantilla, I. D.; Cristancho, D. E.; Ejaz, S.; Hall, K. R.; Atilhan, M.; Iglesias-Silva, G. A. P-ρ-T data for carbon dioxide from (310 to 450) K up to 160 MPa. *J. Chem. Eng. Data* **2010**, *55* (11), 4611−4613.

(25) Pattabiraman, V. R.; Bode, J. W. Rethinking amide bond synthesis. *Nature* **2011**, *480* (7378), 471−479.

(26) Patel, H. A.; Yavuz, M. S.; Yavuz, C. T. Exceptional organic solvent uptake by disulfide-linked polymeric networks. *RSC Adv.* **2014**, *4* (46), 24320−24323.

(27) Worzakowska, M. TG/FTIR/QMS studies of long chain esters of geraniol. *J. Anal. Appl. Pyrolysis* **2014**, *110* (0), 181−193.

(28) Young, S. K.; Gemeinhardt, G. C.; Sherman, J. W.; Storey, R. F.; Mauritz, K. A.; Schiraldi, D. A.; Polyakova, A.; Hiltner, A.; Baer, E. Covalent and non-covalently coupled polyester−inorganic composite materials. *Polymer* **2002**, *43* (23), 6101−6114.

(29) Patel, H. A.; Sang, H. J.; Park, J.; Chen, D. P.; Jung, Y.; Yavuz, C. T.; Coskun, A. Unprecedented high-temperature CO2 selectivity in N2-phobic nanoporous covalent organic polymers. *Nat. Commun.* **2013**, *4*, 1357.

(30) Mason, C. R.; Maynard-Atem, L.; Heard, K. W. J.; Satilmis, B.; Budd, P. M.; Friess, K.; Lanč, M.; Bernardo, P.; Clarizia, G.; Jansen, J. C. Enhancement of CO2 Affinity in a Polymer of Intrinsic Microporosity by Amine Modification. *Macromolecules* **2014**, *47* (3), 1021−1029.

(31) Sun, Z.; Li, Y.; Guan, X.; Chen, L.; Jing, X.; Xie, Z. Rational design and synthesis of covalent organic polymers with hollow structure and excellent antibacterial efficacy. *RSC Adv.* **2014**, *4* (76), 40269−40272.

(32) Chiou, K.; Hollanger, E.; Agag, T.; Ishida, H. Highly Improved Thermal Properties of Hydroxyl-Containing Polymers via Modification by Benzoxazine Groups. *Macromol. Chem. Phys.* **2013**, *214*, 1629−1635.

(33) Dawson, R.; Cooper, A. I.; Adams, D. J. Nanoporous organic polymer networks. *Prog. Polym. Sci.* **2012**, *37* (4), 530−563.

(34) Thi, T. H.; Matsusaki, M.; Hirano, H.; Kawano, H.; Agari, Y.; Akashi, M. Mechanism of high thermal stability of commercial polyesters and polyethers conjugated with bio-based caffeic acid. *J. Polym. Sci., Part A: Polym. Chem.* **2011**, *49* (14), 3152−3162.

DOI: 10.1021/acsami.6b05927
ACS Appl. Mater. Interfaces 2016, 8, 20772−20785

(35) Seredych, M.; Jagiello, J.; Bandosz, T. J. Complexity of CO2 adsorption on nanoporous sulfur-doped carbons − Is surface chemistry an important factor? *Carbon* **2014**, *74* (0), 207−217.
(36) Kipling, J. J.; Sherwood, J. N.; Shooter, P. V.; Thompson, N. R. The pore structure and surface area of high-temperature polymer carbons. *Carbon* **1964**, *1* (3), 321−328.
(37) Meng, L.-Y.; Park, S.-J. MgO-templated porous carbons-based CO2 adsorbents produced by KOH activation. *Mater. Chem. Phys.* **2012**, *137* (1), 91−96.
(38) Rouquerol, F.; Rouquerol, J.; Sing, K. Interpretation of Physisorption Isotherms at the Gas-Solid Interface. In *Adsorption by Powders and Porous Solids*; Rouquerol, F., Rouquerol, J., Sing, K., Eds.; Academic Press: London, 1999; Chapter 4, pp 93−115.
(39) Xiang, Z.; Cao, D.; Wang, W.; Yang, W.; Han, B.; Lu, J. Postsynthetic Lithium Modification of Covalent-Organic Polymers for Enhancing Hydrogen and Carbon Dioxide Storage. *J. Phys. Chem. C* **2012**, *116* (9), 5974−5980.
(40) Xiang, Z.; Cao, D. Synthesis of Luminescent Covalent−Organic Polymers for Detecting Nitroaromatic Explosives and Small Organic Molecules. *Macromol. Rapid Commun.* **2012**, *33* (14), 1184−1190.
(41) Ben, T.; Ren, H.; Ma, S.; Cao, D.; Lan, J.; Jing, X.; Wang, W.; Xu, J.; Deng, F.; Simmons, J. M.; Qiu, S.; Zhu, G. Targeted Synthesis of a Porous Aromatic Framework with High Stability and Exceptionally High Surface Area. *Angew. Chem., Int. Ed.* **2009**, *48* (50), 9457−9460.
(42) Yuan, D.; Lu, W.; Zhao, D.; Zhou, H.-C. Highly Stable Porous Polymer Networks with Exceptionally High Gas-Uptake Capacities. *Adv. Mater.* **2011**, *23* (32), 3723−3725.
(43) Boot-Handford, M. E.; Abanades, J. C.; Anthony, E. J.; Blunt, M. J.; Brandani, S.; Mac Dowell, N.; Fernandez, J. R.; Ferrari, M.-C.; Gross, R.; Hallett, J. P.; Haszeldine, R. S.; Heptonstall, P.; Lyngfelt, A.; Makuch, Z.; Mangano, E.; Porter, R. T. J.; Pourkashanian, M.; Rochelle, G. T.; Shah, N.; Yao, J. G.; Fennell, P. S. Carbon capture and storage update. *Energy Environ. Sci.* **2014**, *7* (1), 130−189.
(44) Walton, K. S.; Millward, A. R.; Dubbeldam, D.; Frost, H.; Low, J. J.; Yaghi, O. M.; Snurr, R. Q. Understanding Inflections and Steps in Carbon Dioxide Adsorption Isotherms in Metal-Organic Frameworks. *J. Am. Chem. Soc.* **2008**, *130* (2), 406−407.
(45) Del Regno, A.; Gonciaruk, A.; Leay, L.; Carta, M.; Croad, M.; Malpass-Evans, R.; McKeown, N. B.; Siperstein, F. R. Polymers of Intrinsic Microporosity Containing Tröger Base for CO2 Capture. *Ind. Eng. Chem. Res.* **2013**, *52* (47), 16939−16950.
(46) Montagnaro, F.; Silvestre-Albero, A.; Silvestre-Albero, J.; Rodríguez-Reinoso, F.; Erto, A.; Lancia, A.; Balsamo, M. Post-combustion CO2 adsorption on activated carbons with different textural properties. *Microporous Mesoporous Mater.* **2015**, *209*, 157−164.
(47) Arena, F.; Italiano, G.; Barbera, K.; Bordiga, S.; Bonura, G.; Spadaro, L.; Frusteri, F. Solid-state interactions, adsorption sites and functionality of Cu-ZnO/ZrO2 catalysts in the CO2 hydrogenation to CH3OH. *Appl. Catal., A* **2008**, *350* (1), 16−23.
(48) Yang, S.; Sun, J.; Ramirez-Cuesta, A. J.; Callear, S. K.; David, W. I. F.; Anderson, D. P.; Newby, R.; Blake, A. J.; Parker, J. E.; Tang, C. C.; Schröder, M. Selectivity and direct visualization of carbon dioxide and sulfur dioxide in a decorated porous host. *Nat. Chem.* **2012**, *4* (11), 887−894.
(49) Wang, H.; Qu, Z. G.; Zhang, W.; Chang, Y. X.; He, Y. L. Experimental and numerical study of CO2 adsorption on Ni/DOBDC metal-organic framework. *Appl. Therm. Eng.* **2014**, *73* (2), 1501−1509.
(50) Liu, Y.; Wilcox, J. Effects of Surface Heterogeneity on the Adsorption of CO2 in Microporous Carbons. *Environ. Sci. Technol.* **2012**, *46* (3), 1940−1947.
(51) Pan, Y.-x.; Liu, C.-j.; Mei, D.; Ge, Q. Effects of Hydration and Oxygen Vacancy on CO2 Adsorption and Activation on β-Ga2O3(100). *Langmuir* **2010**, *26* (8), 5551−5558.
(52) Plaza, M. G.; Pevida, C.; Arenillas, A.; Rubiera, F.; Pis, J. J. CO2 capture by adsorption with nitrogen enriched carbons. *Fuel* **2007**, *86* (14), 2204−2212.
(53) Pan, H.; Ritter, J. A.; Balbuena, P. B. Examination of the Approximations Used in Determining the Isosteric Heat of Adsorption from the Clausius−Clapeyron Equation. *Langmuir* **1998**, *14* (21), 6323−6327.
(54) Krungleviciute, V.; Migone, A. D.; Yudasaka, M.; Iijima, S. CO2 Adsorption on Dahlia-Like Carbon Nanohorns: Isosteric Heat and Surface Area Measurements. *J. Phys. Chem. C* **2012**, *116* (1), 306−310.
(55) Esteves, I. A. A. C.; Lopes, M. S. S.; Nunes, P. M. C.; Mota, J. P. B. Adsorption of natural gas and biogas components on activated carbon. *Sep. Purif. Technol.* **2008**, *62* (2), 281−296.
(56) Demessence, A.; D'Alessandro, D. M.; Foo, M. L.; Long, J. R. Strong CO2 Binding in a Water-Stable, Triazolate-Bridged Metal−Organic Framework Functionalized with Ethylenediamine. *J. Am. Chem. Soc.* **2009**, *131* (25), 8784−8786.
(57) Dunne, J. A.; Mariwala, R.; Rao, M.; Sircar, S.; Gorte, R. J.; Myers, A. L. Calorimetric Heats of Adsorption and Adsorption Isotherms. 1. O2, N2, Ar, CO2, CH4, C2H6, and SF6 on Silicalite. *Langmuir* **1996**, *12* (24), 5888−5895.
(58) Reich, T.; El-Kaderi, H. Impact of tailored chemical and textural properties on the performance of nanoporous borazine-linked polymers in small gas uptake and selective binding. *J. Nanopart. Res.* **2013**, *15*, 1368.
(59) Awadallah-F, A.; Al-Muhtaseb, S. Carbon dioxide sequestration and methane removal from exhaust gases using resorcinol−formaldehyde activated carbon xerogel. *Adsorption* **2013**, *19* (5), 967−977.
(60) Aroonwilas, A.; Tontiwachwuthikul, P. Mass Transfer Coefficients and Correlation for CO2 Absorption into 2-Amino-2-methyl-1-propanol (AMP) Using Structured Packing. *Ind. Eng. Chem. Res.* **1998**, *37* (2), 569−575.
(61) Bao, Z.; Yu, L.; Ren, Q.; Lu, X.; Deng, S. Adsorption of CO2 and CH4 on a magnesium-based metal organic framework. *J. Colloid Interface Sci.* **2011**, *353* (2), 549−556.
(62) Yim, W.-L.; Byl, O.; Yates, J. T.; Johnson, J. K. Vibrational behavior of adsorbed CO2 on single-walled carbon nanotubes. *J. Chem. Phys.* **2004**, *120* (11), 5377−5386.
(63) Mishra, A. K.; Ramaprabhu, S. Study of CO_2 Adsorption in Low Cost Graphite Nanoplatelets. *Int. J. Chem. Eng. Appl.* **2010**, *1* (3), 266.
(64) Köck, E.-M.; Kogler, M.; Bielz, T.; Klötzer, B.; Penner, S. In Situ FT-IR Spectroscopic Study of CO2 and CO Adsorption on Y2O3, ZrO2, and Yttria-Stabilized ZrO2. *J. Phys. Chem. C* **2013**, *117* (34), 17666−17673.

DOI: 10.1021/acsami.6b05927
ACS Appl. Mater. Interfaces 2016, 8, 20772−20785